A Novel Dual-Band Rectifier Circuit with Enhanced Bandwidth for RF Energy Harvesting Applications

Tologon Karataev[1], Adrian Bekasiewicz[1]
[1] Faculty of Electronics, Telecommunications and Inf.
Gdansk University of Technology
Gdansk, Poland
tolkarat@pg.edu.pl, bekasiewicz@ru.is

Slawomir Koziel[1,2]
[2] Engineering Optimization & Modeling Center
Reykjavik University
Reykjavik, Iceland
koziel@ru.is

Abstract—**In recent years, a rapid development of low-power sensor networks, enabling machine-to-machine communication in applications such as environmental monitoring, has been observed. Contemporary sensors are normally supplied by an external power source, typically in a form of a battery, which limits their lifespan and increases the maintenance costs. This problem can be addressed by harvesting and converting ambient RF energy into DC power. In the paper, a novel dual-band rectifier circuit with high efficiency and enhanced bandwidth for RF energy harvesting applications is proposed along with its design procedure. The rectifier consists of two branches fed through a junction and two voltage doublers with a common DC output. The proposed structure is designed to work in 0.6 GHz to 1 GHz and 1.75 GHz to 2.45 GHz ranges with an average RF-to-DC conversion efficiency of at least 50 percent. Compact dimensions of 19 mm × 17 mm (a footprint of only 345 mm^2) have been obtained through appropriate folding of the impedance transformers. As demonstrated, the proposed design outperforms state-of-the-art rectifiers in terms of the operational bandwidth, efficiency, and the range of acceptable load impedances.**

Keywords—Ambient energy harvesting; rectifier circuit; voltage doubler; efficient microwave-to-DC conversion; compact rectifier

I. INTRODUCTION

Increased market demand for sensor networks for Internet of Things, or machine-to-machine communications, stimulates the research on highly-integrated sensors that can operate in various environments [1]. In this context, development of efficient circuits for ambient RF energy harvesting, where power from electromagnetic sources can be converted into direct current (DC), gained significant attention [1]-[6]. The harvesting structure is composed of an antenna which receives the ambient energy, and a rectifier circuit [7]. A typical rectifier consists of an RF-to-DC converter, an impedance transformer between the circuit and the antenna, and a DC filter for smoothing the output voltage. Converters are normally implemented using low-biased diodes, such as Schottky ones [2]. Schottky diodes exhibit low threshold voltage and relatively low junction capacitance, both necessary for obtaining high efficiency at low input power levels, and for increasing the operating frequency [2]. The DC filters are implemented using either lumped and distributed components. The latter, however, significantly contribute to the rectifier size [2], [6], [8].

Conventional rectifiers implemented in planar or CMOS technology are normally characterized by narrow operational bandwidth and high conversion efficiency of up to 80% [9], [10]. On the other hand, variability and low levels of ambient energy result in limited applicability of such circuits [6]. To mitigate this problem, a rectifier can be supplied by an antenna array [4], [11]. However, large sizes of array structures become problematic for space limited applications. Alternatively, reconfigurable DC-converters with a few diodes adjusted for various input power levels can be used [6]. In any case, single-frequency harvesters may be incapable of providing sufficient energy for reliable sensor operation.

To take advantage of availability of RF energy in a broad spectrum, modern rectifiers are often characterized by multi-band [6], [11] or wideband operation [1], [2]. The greatest challenge related to design of such structures is to match the impedance of a DC-converter to the RF input within the frequency range of interest. This is normally achieved using multi-stage distributed-component networks, which increases the size and complexity of the rectifier [4], [12]. Another problem is that multi-band rectifiers can cover the range of up to 100 MHz, which is narrow compared to the spectrum covered by, e.g., cellular, or WiFi transmitters [13]. On the other hand, bandwidth-enhanced circuits are often characterized by poor in-band reflection and/or relatively low efficiency [1], [2].

The above considerations indicate that reliable rectifier circuits for RF energy harvesting should provide high conversion efficiency within a range of frequencies covered by the systems with multiple broadcasting stations (preferably cellular, TV, and, in urban areas, WiFi). Also, the structure should be compact and—to increase the RF power level at the input of DC-converter—feature a decent in-band matching. Here, these characteristics are achieved by a proposed novel dual-band rectifier with enhanced bandwidth. The structure consists of two voltage doublers with a common DC output. Each converter is fed through a separate broadband impedance transformer connected to a T-junction with 50 Ω input impedance. Compact rectifier dimensions of 19 mm × 17 mm have been obtained through appropriate folding of its matching circuits. The structure is designed to work in 0.6 GHz to 1 GHz and 1.75 GHz to 2.45 GHz bands, which covers the operational ranges of the systems mentioned above. Depending on the input

power level and load resistance, an average in-band conversion efficiency of the proposed structure is up to 63 percent, with the maximum in-band reflection being below –10 dB. The proposed structure outperforms other state-of-the-art rectifiers in terms of efficiency, operational bandwidth, and the range of acceptable load impedances.

II. DUAL-BAND RECTIFIER WITH ENHANCED BANDWIDTH

In this section, we explain the design process of the proposed dual-band rectifier. In particular, we describe the utilized converter configuration, design of single-band circuits, as well as the assembly and adjustment of the structure parameters. The computational models are implemented using a Keysight ADS harmonic balance simulator (circuit model) [15]. Rectifier miniaturization and its electromagnetic (EM) tuning are considered in Section III. Simulation results and comparisons with benchmark rectifiers are discussed in Section IV.

A. Problem Formulation and Design Specifications

The design problem if formulated as the following minimization task:

$$x^* = \arg\min_x U(R(x)) \qquad (1)$$

where, R is the response of the structure under optimization (equivalent-circuit or EM model, depending on the design stage), U is the scalar objective function, whereas x represents the vector of adjustable parameters; x^* is the optimal design to be found. The following set of design specifications has been assumed:
- Frequency bands: from 0.6 GHz to 1 GHz and from 1.75 GHz to 2.45 GHz;
- Maximum in-band reflection: –10 dB;
- Minimum average in-band efficiency 50%.

The rectifier efficiency is defined as $\eta = P_{DC}/P_{RF}$, where $P_{DC} = V_L^2/R_L$ and P_{RF} is the RF power at the rectifier input [14], whereas the output voltage and the load impedance are denoted by V_L and R_L, respectively. The design process is performed for $R_L = 5$ kΩ and $P_{RF} = -5$ dBm. It is assumed that the structure should feature compact dimensions and be implemented in the microstrip technology. The substrate is a 0.762 mm thick Taconic RF-35 ($\varepsilon_r = 3.5$, $\tan\delta = 0.0018$).

B. Voltage Doubler

The rectifying circuit is a crucial component of an energy harvester that performs RF-to-DC conversion. Here, a voltage doubler configuration shown in Fig. 1 is used. The converter consists of two diodes connected in series and a shunt configuration interconnected with two capacitors. The latter provide energy storage and filter out low frequencies [2]. The circuit works as follows. For the positive wave cycle, the energy is stored in a shunt capacitor and rectified in a series diode. For the negative cycle, a shunt diode and a series capacitor are used for conversion and storage. It should be noted that the energy stored in the series capacitor can be transferred to the shunt one. This results in approximately two-fold increase of the output voltage compared to a circuit with a single diode configuration (hence, a voltage doubler) [2].

Selection of appropriate components is of key importance for obtaining high-performance of the converter circuit. In this work, we use a Skyworks SMS7630 Schottky diode which provides low forward bias (from 60 mV to 120 mV at 1 mA) for low input power signals. We also use 100 nF Murata chip capacitors which provide effective short circuits in the frequency bands of interest [1], [2].

C. Single-Band Rectifiers with Enhanced Bandwidth

The input impedance of the voltage doubler of Section II.C is characterized by a large imaginary component which has to be compensated. It has been achieved, at the center frequency of the selected band, using a series lumped inductor. The low-imaginary-part complex impedance can be then matched to 50 Ω using a non-uniform-transmission-line-based microstrip transformer (here, tapered lines are used).

The design procedure for a single-band matching circuit consists of three steps: (i) compensate imaginary part of the voltage doubler input impedance using a series inductor, (ii) synthesize the matching transformer topology, and (iii) approximate the obtained electrical parameters using non-uniform transmission lines and optimize the transformer structure. Here, the impedance transformer is synthesized based on the Klopfenstein taper formulas [16]. It should be noted that utilization of non-uniform transformers is preferable, due to their usefulness for obtaining wideband impedance matching for resistive loads. Moreover, they are suitable for obtaining broadband matching for complex loads characterized by relatively low imaginary parts [1]. Conceptual illustration of the matching circuit used here has been shown in Fig. 2.

The above design procedure has been applied to design of the matching circuits for both single-band structures. The input impedance of the rectifier at $f_1 = 0.8$ GHz (center frequency for the lower-band) is $Z_{in.1}^{(0)} = 145 - j328$ Ω. The imaginary part has been compensated (Step I) using a 51 nH series inductor manufactured by Murata (see Fig. 2). The resulting impedance of $Z_{in.1}^{(1)} = 147 - j14$ Ω has been then matched using a four section transformer (Step II). The electrical parameters of the synthesized circuit $Z_1 = 58.3$ Ω, $Z_2 = 76.2$ Ω, $Z_3 = 98$ Ω, $Z_4 = 121.7$ Ω, and $\theta = 33.9°$ have been used to determine dimensions of the non-uniform transformer and the structure has been optimized to minimize its in-band reflection (Step III). The structure parameter vector is $x = [w_1\ w_2\ w_3\ w_4\ l_1\ l_2\ l_3\ l_4]^T$ mm, whereas $w_0 = 1.7$ mm. The optimized dimensions are $x_1^* = [0.2\ 0.56\ 0.2\ 0.2\ 24.5\ 4.05\ 25.93\ 27.58]^T$. Reflection characteristics at each stage of the impedance transformer design are shown in Fig. 3(a).

The center frequency for the higher-band rectifier is $f_2 = 2.1$ GHz. The corresponding input impedance is $Z_{in.2}^{(0)} = 30 - j120$. The reactance has been compensated using a 7.5 nH inductor. The impedance is $Z_{in.2}^{(1)} = 38 - j25.6$ Ω. The synthesized impedance transformer consists of four sections. Its electrical parameters $Z_1 = 48.6$ Ω, $Z_2 = 45.4$ Ω, $Z_3 = 41.9$ Ω, $Z_4 = 39.3$ Ω, and $\theta = 47.2°$ have been utilized to obtain the starting point for reflection optimization of the non-uniform-lines-based transformer. The vector of optimized parameters is $x_2^* = [1.59\ 3.44\ 3.93\ 1.73\ 15.46\ 13.5\ 14.32\ 25.66]^T$ mm (cf. Fig. 2). Reflection characteristics of the upper-band matching circuit at each stage of the design process are given in Fig. 3(b).
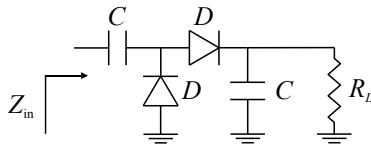
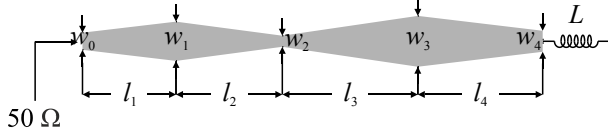Fig. 1. Schematic diagram of used voltage doubler circuit.

50 Ω

Fig. 2. Rectifier matching circuit composed of non-uniform transmission lines and the series inductor: conceptual illustration.

D. Design of Dual-Band Rectifier

The proposed rectifier circuit consists of two (lower- and upper-band) branches with a common RF input and DC output. Upon assembly, the design parameters of the distributed component-based networks in both branches have been tuned to improve the in-band matching. The dimensions of the optimized impedance transformers of the dual-band rectifier are $x_{r1}^* = $ [0.2 2.23 0.59 0.2 10.1 9.68 7.36 55.5]^T and $x_{r2}^* = $ [1.14 3.13 3.26 0.21 2.54 1.1 1.02 0.52]^T for lower- and upper-band branch, respectively. The reflection characteristics of the structure before and after tuning are compared in Fig. 4(a). The response of the tuned design slightly violates the requirement concerning –10 dB in-band impedance. However, this will be improved in the course of structure miniaturization (cf. Section III).

It is worth mentioning that the matching circuits of both branches exhibit band-pass characteristics (see Fig. 3). Therefore, from the RF perspective, the structure is a diplexer that increases isolation between the branches at the converter inputs. As a result, high rectifier efficiency along with low in-band reflection can be obtained for both bands. This is important to ensure a possibly high power level at the DC output of the structure.

III. RECTIFIER MINIATURIZATION AND EM-BASED TUNING

The rectifier is of Section II.D is characterized by large dimensions of 60 mm × 20 mm (footprint: 1200 mm²). To make the design more compact, both its impedance transformers have been folded as shown in Fig. 5. The vector of miniaturized structure parameters is $x = [w_{11} \; w_{12} \; w_{13} \; l_{15} \; l_{12} \; l_{16} \; l_{18} \; w_t \; w_{21} \; w_{22} \; w_{23} \; l_{23} \; l_{22} \; l_{21}]^T$, whereas dimensions $w_0 = 1.7$, $l_{11} = 2$, $l_{19} = 1$ are fixed. Relative variables are $l_{13} = 2l_{19} + l_{12}$, $l_{14} = 2l_{19} + 0.5w_{12}$, $l_{110} = 1/3 \cdot l_{18}$, $l_{111} = \mathrm{abs}(0.5w_{21} + l_{21} + w_0 + l_{11} + 2.5w_{11} + l_{12} - 6w_{13} - 3.92)$, and $l_{112} = \mathrm{abs}(l_{18} - \mathrm{abs}(l_{15} + l_{16} + 0.5w_{11} + 0.5w_{13} - l_{22} - l_{23} - 0.5w_{21}) + 0.5w_{13})$. The unit for all parameters is mm. Line widths of the rectifier DC part are set to 1 mm.

The distributed component network of the miniaturized rectifier is implemented in Momentum EM simulator (mesh density: 50 cells per wavelength). Its S-parameter-based model is interconnected in a circuit simulator with diodes and lumped elements. The resulting co-simulation model was used for accurate performance evaluation. The initial design of the structure, obtained based on dimensions of the rectifier of Section II.D, is $x = $ [0.2 2.23 0.2 9.67 1.33 7.36 14.21 1.7 1.23

3.21 0.21 0.52 3.92 2.29]^T. The structure was optimized for improved matching and efficiency within the frequency bands of interest (cf. Section II.A). The final design is $x^* = $ [0.2 2.48 0.21 9.71 1.96 7.71 13.2 2.44 2.33 3.5 0.21 0.39 2.73 1.74]^T. A comparison of rectifier reflection characteristics at the initial and optimized designs is shown in Fig. 4(b). Dimensions of the optimized structure are 19 mm × 17.1 mm and its footprint is only 325 mm², 73% smaller compared to conventional rectifier. The structure frequency range of operation—for the –10 dB in-band reflection—is from 0.56 GHz to 1.06 GHz and from 1.75 to 2.55 GHz.

IV. RESULTS AND COMPARISONS

The efficiency figures of the proposed rectifier for various input power levels are shown in Fig. 6. For $P_{RF} = –5$ dBm, the lower- and upper-band average efficiency is 57.1% and 52.3%, respectively, whereas the average efficiency for input power of –10 dBm and 0 dBm is above 38 % and 61 % (for both bands). Figure 7 shows the rectifier reflection and efficiency responses versus frequency for $P_{RF} = –5$ dBm and a range of loads between 2 kΩ to 12 kΩ. The maximum in-band reflection and average efficiency for the considered loads varies from –10 dB to –7.3 dB and from 40% to 57%, respectively.

The proposed structure has been benchmarked against state-of-the-art rectifiers reported in the literature. The figures of interest are (i) reflection-wise bandwidth (BW) and in-band reflection level, (ii) average in-band efficiency for –10 dBm input power, and (iii) load range for which in-band efficiency is greater than 40 % (for maximum η vs. P_{RF}). The results in Table I indicate that the proposed structure outperforms other rectifiers in terms of all listed performance figures.
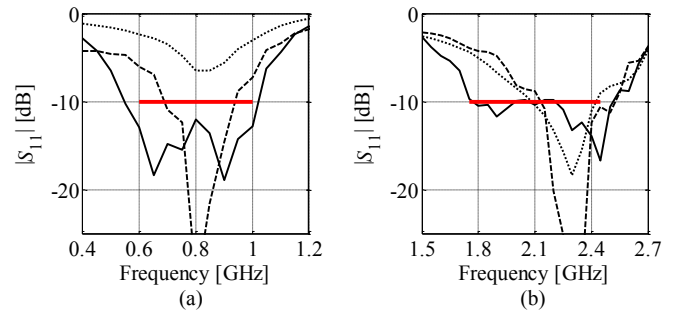

Fig. 3. Reflection characteristics of rectifiers operating at: (a) lower- and (b) upper-band at step I (·····), II (– –), and III (——) of matching circuits development.
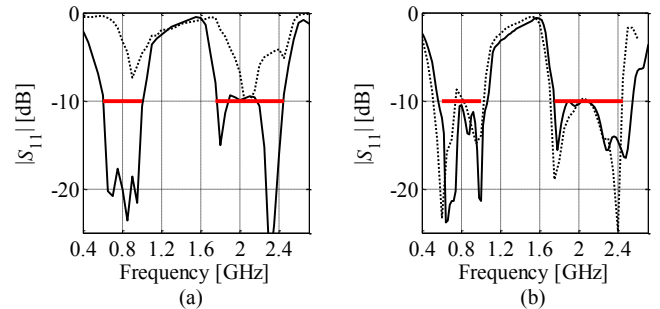

Fig. 4. Reflection characteristics of the dual-band rectifiers at initial (·····) and optimized (——) designs: (a) conventional (circuit model simulations) and (b) miniaturized circuit (EM model simulations).
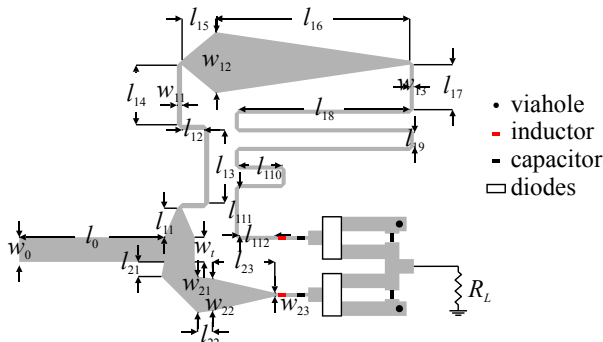
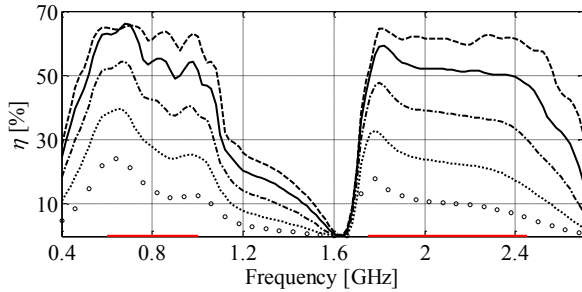Fig. 5. Geometry of the proposed rectifier circuit.

Fig. 6. Efficiency of the optimized rectifier circuit for PRF of –20 dBm (○○), –15 dBm (····), –10 dBm (·–·), –5 dBm (—), and 0 dBm (– –).
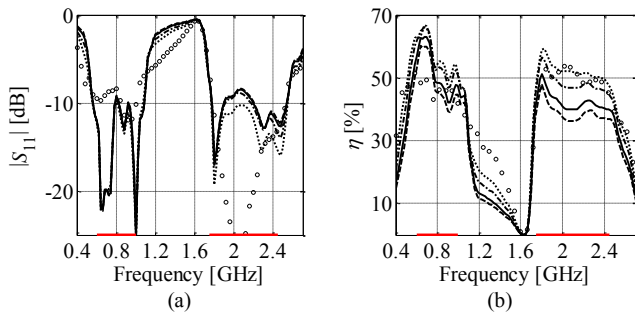

Fig. 7. Comparison of rectifier responses for input power level of –5 dBm and load impedance of 2 kΩ (○○), 5 kΩ (····), 7 kΩ (·–·), 10 kΩ (—), and 12 kΩ (– –): (a) reflection characteristics, and (b) efficiency.

TABLE I COMPARISON WITH BENCHMARK RECTIFIERS

Circuit	BW [MHz]	max(S_{11}) in-band [dB]	avg(η) [%]	R_L range [kΩ] min(η) > 40%	BW [GHz] min(η) > 40%
[6]	100, 50, 150, 100	–5	50, 35, 40, 35	N/A	0.85 - 0.95, 1.25-1.3, 1.95 - 2.05, N/A
[2]	700	–5	45	N/A	1.8 – 2.5
[1]	500	–6	N/A	5.5 – 12	0.45 – 0.95
[5]	100 700	–5 –5	45 43	0.2 – 2, N/A	0.95 –1.05, 1.8 – 2.15
This work	500 780	–10	45, 39	2 – 12, 2 – 12	0.44 – 1.1, 1.72 – 2.66

V. CONCLUSION

In this paper, a novel compact dual-band rectifier circuit with an enhanced bandwidth and high efficiency has been proposed. The structure consists of two interconnected bandwidth-enhanced rectifiers with a non-uniform-transmission-line-based matching circuit. Compact dimensions of 19 mm × 17.1 mm and a small footprint of 345 mm² have been obtained by folding high-impedance lines of the matching circuits. The proposed rectifier

features a wide impedance bandwidths of 500 MHz and 780 MHz (at –10 dB reflection level), respectively. At the same time, the efficiency above 40% is obtained within the bands of 620 MHz and 800 MHz, respectively. The structure outperforms the state-of-the-art rectifiers reported in the literature in terms of the reflection- and efficiency bandwidths, as well as acceptable range of load impedances. The future work will focus on experimental validation of the proposed circuit working with a dedicated antenna.

REFERENCES

[1] J. Kimionis, A. Collado, M.M. Tentzeris, and A. Georgiadis, "Octave and decade printed UWB rectifiers based on nonuniform transmission lines for energy harvesting," *IEEE Trans. Microwave Theory Techn.*, vol. 65, no. 11, pp. 4326-4334, 2017.

[2] C. Song, Y. Huang, J. Zhou, J. Zhang, S. Yuan, and P. Carter, "A high-efficiency broadband rectenna for ambient wireless energy harvesting," *IEEE Trans. Ant. Prop.*, vol. 63, no. 8, pp. 3486-3495, 2015.

[3] Q.W. Lin and X.Y. Zhang, "Differential rectifier using resistance compression network for improving efficiency over extended input power range," *IEEE Trans. Microwave Theory Techn.*, vol. 64, no. 9, pp. 2943-2954, 2016.

[4] U. Olgun, C.C. Chen, and J. L. Volakis, "Investigation of rectenna array configurations for enhanced RF power harvesting," *IEEE Ant. Wireless Prop. Lett.*, vol. 10, pp. 262-265, 2011.

[5] C. Song et al., "Matching network elimination in broadband rectennas for high-efficiency wireless power transfer and energy harvesting," *IEEE Trans. Industrial Electronics*, vol. 64, no. 5, pp. 3950-3961, 2017.

[6] J.J. Lu, X.X. Yang, H. Mei, and C. Tan, "A four-band rectifier with adaptive power for electromagnetic energy harvesting," *IEEE Microwave Wireless Comp. Lett.*, vol. 26, no. 10, pp. 819-821, 2016.

[7] C.R. Valenta and G.D. Durgin, "Harvesting wireless power: survey of energy-harvester conversion efficiency in far-field, wireless power transfer systems," *IEEE Microwave Mag.*, vol. 15, no. 4, pp. 108-120, 2014.

[8] K. Niotaki, S. Kim, S. Jeong, A. Collado, A. Georgiadis and M.M. Tentzeris, "A compact dual-band rectenna using slot-loaded dual band folded dipole antenna," *IEEE Ant. Wireless Prop. Lett.*, vol. 12, pp. 1634-1637, 2013.

[9] Y. Huang, N. Shinohara, and T. Mitani, "A constant efficiency of rectifying circuit in an extremely wide load range," *IEEE Trans. Microwave Theory Techn.*, vol. 62, no. 4, pp. 986-993, 2014.

[10] H. Sun, Y. Guo, M. He and Z. Zhong, "Design of a high-efficiency 2.45-GHz rectenna for low-input-power energy harvesting," *IEEE Ant. Wireless Prop. Lett.*, vol. 11, pp. 929-932, 2012.

[11] H. Sun, Y. Guo, M. He, and Z. Zhong, "A dual-band rectenna using broadband Yagi antenna array for ambient RF power harvesting," *IEEE Ant. Wireless Prop. Lett.*, vol. 12, pp. 918-921, 2013.

[12] D. Masotti, A. Costanzo, M.D. Prete, and V. Rizzoli, "Genetic-based design of a tetra-band high-efficiency radio-frequency energy harvesting system," *IET Microwaves, Ant. Prop.*, vol. 7, no. 15, pp. 1254-1263, 2013.

[13] R.J. Vyas, B.B. Cook, Y. Kawahara, and M.M. Tentzeris, "E-WEHP: a batteryless embedded sensor-platform wirelessly powered from ambient digital-TV signals," *IEEE Trans. Microwave Theory Techn.*, vol. 61, no. 6, pp. 2491-2505, 2013.

[14] V. Palazzi et al., "A novel ultra-lightweight multiband rectenna on paper for RF energy harvesting in the next generation LTE bands," *IEEE Trans. Microwave Theory Techn.*, vol. 66, no. 1, pp. 366-379, 2018.

[15] Agilent (Keysight) ADS, ver. 2011.10, Agilent Technologies, 1400 Fountaingrove Parkway, Santa Rosa, CA 95403-1799, 2011.

[16] G. Razmafrouz, G.R. Branner, and B.P. Kumar, "Formulation of the Klopfenstein tapered line analysis from generalized nonuniform line theory," *Proc. Midwest Symp. Circuits Syst.*, pp. 1177-1180, 1996.